Russian Geology and Geophysics © 2021, V.S. Sobolev IGM, Siberian Branch of the RAS
Vol. 62, No. 2, pp. 207–222, 2021 DOI:10.2113/RGG20194099
Geologiya i Geofizika

Causes of the Occurrence of *A*-Type Volcanic Rocks in Active Continental Margins (Southern Sikhote-Alin, Russian Far East)

A.V. Grebennikov✉, S.O. Maksimov

Far East Geological Institute, Far Eastern Branch of the Russian Academy of Sciences, pr. 100-letiya Vladivostoka 159, Vladivostok, 690022, Russia

Received 25 June 2019; accepted 12 February 2020

Abstract—New isotope-geochemical data on the volcanic complexes of the South Yakut and Martel volcanic depressions in southern Primorye are presented. Their formation in the early Eocene (54.3 Ma) and Late Cretaceous (83.5 Ma), respectively, is evidenced by U–Pb zircon dating (LA-ICP-MS). Based on the geochemical characteristics, it is concluded that the volcanics are typical *A*-type igneous rocks. Their formation coincides with the sudden change in the vector of motion of the Pacific slab with respect to the continent in the Campanian and Paleocene–Eocene, which caused destruction of the slab with its probable discontinuity and the injection of the subslab asthenosphere. The effect of mantle fluids on the continental lithospheric-rock melting determined the generation of magmas with the specific geochemical features of *A*-type igneous rocks. The regularities of their composition are due to the deep-seated reduced F-rich fluids that caused the intense differentiation of magmas accumulating fluidized melts enriched in mobile components in the apical part.

Keywords: A-type igneous rocks; fluidal magmatic differentiation; Campanian; Sikhote-Alin

INTRODUCTION

Identifying the relation between igneous processes and geodynamic settings of lithospheric plates' interaction is one of the primary objectives of modern geology. The Pacific Asian margin, particularly the Sikhote-Alin, represents a unique area of the late Mesozoic manifestation of various geodynamic conditions including processes of compression and extension of different scale. The extension processes are associated either with the development of shear deformations caused by intraplate activity (Utkin, 1980, 2005), or with the transform sliding of the oceanic plate with respect to the continental plate followed by a specific magmatism including the *A*-type rocks (Jahn et al., 2015; Kemkin et al., 2016; Martynov et al., 2017; Zhao et al., 2017). The formation of acidic melts of this geochemical type remains quite undetermined (see review Bonin, 2007; Dall'Agnol et al., 2012; Grebennikov, 2014). However, based on the conclusions of most researchers, it was sufficiently demonstrated that they indicate the intracontinental extension caused by a change of the geodynamic regime (from transpression to transtension) (Bonin et al., 1998; Grebennikov et al., 2016; Robinson et al., 2017).

At the same time, the degree to which the igneous rocks of the Sikhote-Alin have been studied by precision analytical methods is not yet high, which often leads to incorrect conclusions on the geochemical characteristics of igneous rocks dependent on the structural permeability of the continental crust.

The article analyses the results of geochronological and geochemical research of volcanic rocks of the southern Sikhote-Alin in order to identify the processes taking place at the level of intermediate chamber, and geodynamic causes of their occurrence. The obtained results were used to propose a mechanism of formation of *A*-type igneous rocks under the conditions of the deep mantle fluids' inflow. These fluids lead to the formation of a specific geochemical type of melts enriched in alkalis. In the process of their generation and evolution major and trace elements are regularly redistributed. We have identified the relation between the formation of *A*-type igneous rocks and the conditions of the large-scale shear dislocations in the background of geodynamic reconstruction of the Pacific margin.

SUBJECTS OF RESEARCH

We investigated extrusive and pyroclastic units of the South Yakut and Martel volcanic depressions (VD) situated in the southern part of the East Sikhote-Alin (Fig. 1).

The South Yakut VD represents a depression type volcanic massif, oval in its shape, up to 14 km in its diameter, separated from host rocks by linear and arc faults. Host rocks are largely interstratified with siliceous members containing Triassic-Jurassic microfossils that are concordantly overlapped mostly by Berriasian–Valanginian sandstone

✉Corresponding author.
E-mail address: greandr@hotmail.com (A.V. Grebennikov)

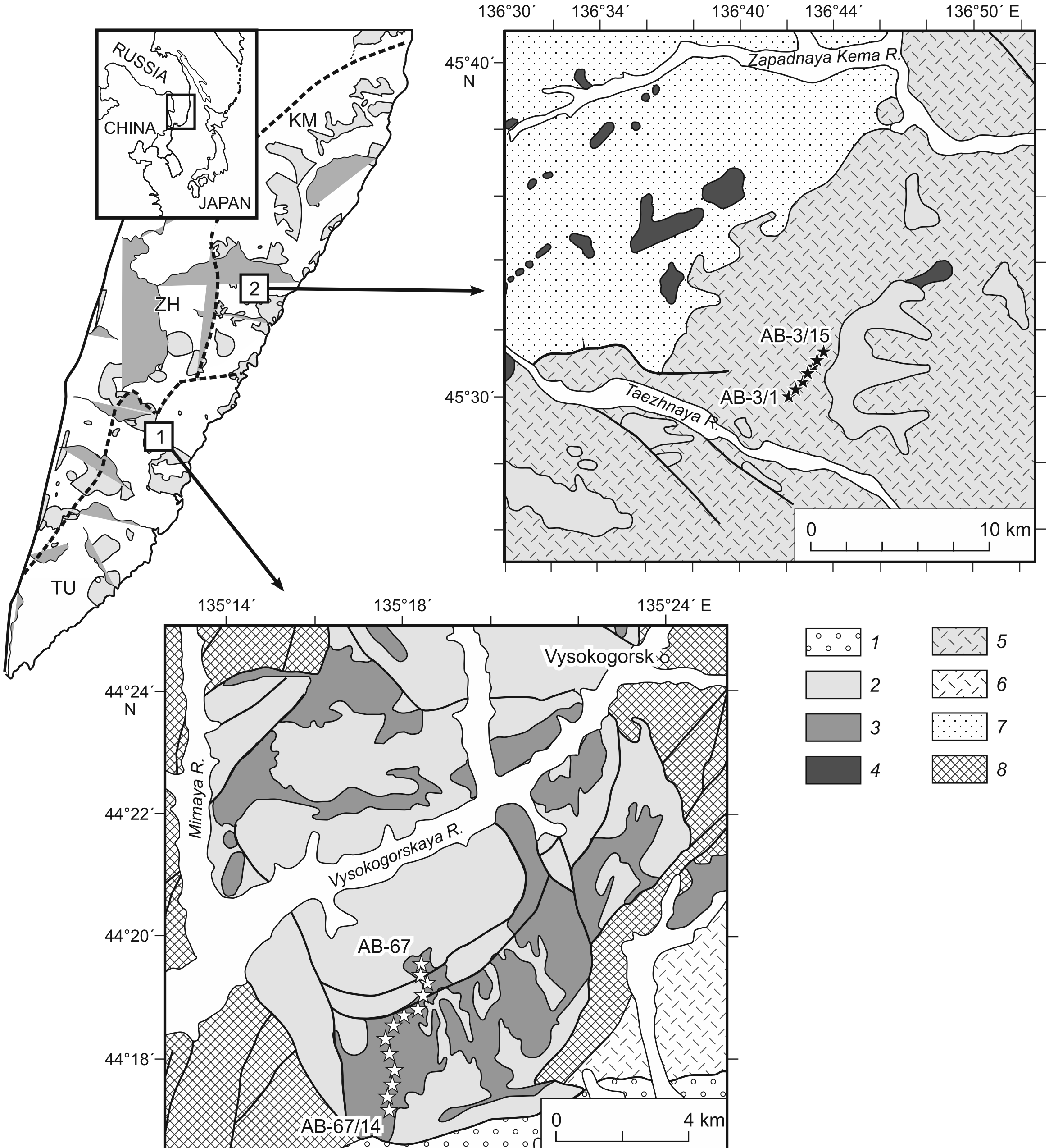

Fig. 1. Simplified geologic map of Cretaceous and Paleogene igneous complexes of the southern Sikhote-Alin. In the inset. Terranes of the late Tithonian–Valanginian accretionary wedge: TU, Taukha; Barremian–early Albian island arc: KM, Kema; Lower Cretaceous turbidite basin: ZH, Zhuravlevka–Amur. Numbers mark volcanic depressions: 1, South Yakut; 2, Martel. Main fields of sedimentary and igneous rocks. *1*, upper Miocene–Pliocene: pebblestones, boulder gravels, loamy sands, loams; *2*, Paleocene: tuffs, ignimbrites of rhyolites and rhyodacites, tuffites; *3*, Paleocene: extrusive rocks of rhyolites, rhyodacites and dacites; *4*, Upper Cretaceous intrusion: granites, granite-porphyries, granodiorites, diorites; *5*, Campanian–Maastrichtian: lithic tuffs and rhyolitic ignimbrites, tuffites, tuffstones, agglomerate tuffs; *6,* Coniacian–Santonian: tuffs and ignimbrites of rhyolites, rhyodacites, and dacites, seams of andesidacites, andesites and their tuffs, tuffites, tuffstones; *7*, Lower Cretaceous: sandstones, silstones, conglomerates, limestones, tuffites, tuffs and tuffstones of the KM terrane; *8,* Triassic–Jurassic: sandstones, less frequently silstones breccia, cherts, siliceous shales, basalts of the TU terrane. Asterisks mark sampling locations.

turbidites (a fragment of the Early Cretaceous accretionary wedge of the Taukha terrane). Olistostrome up to 1100 m thick with blocks and slices of the Paleozoic and early Mesozoic limestones, cherts, basalts and sedimentary rocks was recognized in the roof of the sections (Khanchuk, 2006 and references therein).

According to A.P. Matyunin (1988), the South Yakut VD is made up of volcanic complex, the stratotype of which was distinguished in 1955 (Siyanov Spring, left tributary of Zerkalnaya River) by R.I. Sokolov and E.V. Bykovskaya (Sidorenko, 1969). Overlying rocks are combined into the Siyanovka Formation consisting of two subformation. The lower subsuite is made up of ignimbrites and welded tuffs of biotite rhyolites and rhyodacites, less frequently of tuffites and agglomerate rhyolitic tuffs. The upper subformation includes tuffs, ignimbrites of rhyodacites and dacites. Several findings of relative paleofloral complexes helped to date its age as Maastrichtian (Nazarenko and Bazhanov, 1989). However, S.I. Nevolina pointed to the preliminary character of such definitions and concluded that floral deposits might pertain to the Paleocene (Sidorenko, 1969, p. 308). E.V. Bykovskaya et al. (1960) performed K/Ar dating of rocks for the studied region and established the age of 53–49 Ma.

Linear and concentric arrangement of most intrusive bodies of the South Yakut VD underlines the internal structure of isometric collapse calderas and mainly fissure (along ring faults) type of conduits. Extensive development of pyroclastic units, prevalence of fluidal and spherolitic textures in volcanic rocks, abundance of miarolitic cavities in lavas and in spherulites point to the saturation of the primary magmas in volatile components. The South Yakut VD is an open magmatic system, in which the development of an ignimbrite-forming chamber results in explosion and discharge of melt and fluid components to the surface. Subvolcanic and extrusive units of final magmatic stages belong to the conventionally closed (transition) systems characterized by more developed processes of the shallow magma differentiation, separation of volatile components and metasomatic processes (Popov and Grebennikov, 1997). It should be noted that gold-silver and beryllium-fluorite ore occurrences have been localized in the surrounding area of the volcanic depression (Kovalenko et al., 1968).

The Martel VD, among others, belongs to the vast (its surface is around 5000 km^2) Terney-Kema volcanic field (Vetrennikov, 1976) and forms a part of Solontsovsky paleovolcano. It is placed within the Kema terrane which is a fragment of the Early Cretaceous back-arc basin made up of Barremian-Albian sedimentary, mainly flysch deposits altogether with volcanic rocks of basic and, much less frequently, intermediate or acidic composition (Malinovsky et al., 2002).

The Terney-Kema volcanic field is built up of rocks of various age and composition (e.g., Khanchuk, 2006 and references therein). The Late Cretaceous volcanic rocks of the Martel VD are represented by tuffs and ignimbrites of rhyolites and rhyodacites. The clastic fraction consists of quartz, feldspar, biotite, single grains of amphibolized pyroxene, as well as of lithic (andesites, dacites, rhyolites) and volcanic glass. Extrusive rocks build up a small number of dike bodies and vents, and are represented by fluidal and spherulitic rhyolites, rarely by perlites.

The activity of Solontsovsky paleovolcano that formed c. 80 Ma is registered by the deposits of pyroclastic breccia overlapped by a thick stratum of pyroclastics derived from glowing clouds (Vetrennikov, 1976). The ensuing rhyolitic lava flow entailed the formation of a spreading dome (Panichev et al., 2012).

RESEARCH METHODS

All analytical studies were carried out in the Primorsky Center of Local Elemental and Isotopic Analysis of FEGI FEB RAS, Vladivostok.

U–Pb (isotope) zircon dating. Isotopic measurements were performed using the LA-ICP-MS on Agilent 7500a, coupled with laser ablation system UP-213. Accessory zircon was separated from the samples using the standard method. Final zircon selection was done manually using the binocular microscope. In order to select particular sections for dating we have used the transmitted- and reflected-light, BSE and CLI images of zircons that show the internal structure, zonation, jointing, inclusions.

The measured values were processed by the “Glitter v. 4.4.2” software (Access Macquarie Ltd). U–Pb – ratios were normalized to correspond to the values of isotopic ratios of TEMORA-2, 91500 standard zircons, the ages of which were taken as 416.8 (Black et al., 2004) and 1065.4 Ma (Wiedenbeck et al., 1995) respectively.

Ionometric determination of fluorine. The distinctive feature of the method used to determine fluorine (F) consists in precipitation of interfering elements (Al, Th, Be, REE, etc.) by the means of a $FeCl_2$ solution. The samples were preliminary fused with $KNaCO_3$ at the temperature of 850 ºC and leached by hot distilled water. Filtrate aliquots (25 ml) were neutralized by HCl (1:1), the necessary pH 5.5 was obtained by the addition of an acetate buffer solution. Fluoride-ion concentration was measured using the IONOMETER I-500. Ionometric determination of F was performed with the use of ELIT-221 fluoride electrode and EAL-1M3.1 auxiliary chloride-silver electrode. The relative error for this method was not more than 10%, which is acceptable when F-ion content is low.

Whole-rock major and trace elements. The geochemical determinations were carried out by standard methods of atomic emission spectroscopy with inductively coupled plasma (ICP-AES), mass-spectrometry with inductively coupled plasma (ICP-MS). The determination of major elements of the studied samples in oxide equivalent was performed using ICP-AES on a iCAP 6500 Duo spectrometer (Thermo Scientific, USA) with the addition of cadmium solution (10 ppm concentration) as internal standard. The determinations of H_2O^- and SiO_2 were performed using gravimetry, the contents of ferrous oxide (FeO) using the titrimetry (T). The trace elements were determined using ICP-MS on a Agilent 7500c spectrometer (Agilent Technologies, USA) and taking ^{115}In and ^{209}Bi as internal standards given their final concentration in the solution is 10 ppb.

ANALYTICAL RESULTS

Zircon U–Pb geochronology. At the South Yakut VD extrusive formations, crystal tuffs and rhyolitic ignimbrites supposedly of the final stage of the early Paleogene magmatism of the Southern Sikhote-Alin have been studied. The separated zircon grains are represented by transparent colorless idiomorphic crystals. Some of them of elongated prismatic and dipyramidal shape having elongation indices of 1.5–3, while other zircons are clasts of different size varying from 50 to 100 μm. The CL images of zircons show concentric zonation for most grains and their clasts.

The obtained isotopic data and weighted average U–Pb ages are given in the Table S1 (see Supplementary material in http://sibran.ru/journals/Dop_materials.doc) and in Fig. 2*a–b*. The weighted average U–Pb age of a sample from the South Yakut VD (AB-67/14) is 54.3 ± 2.9 Ma (Eocene: Ypresian). The age of the sample AB-67/6 from the middle part of the pyroclastic section of the VD is 52.2 ± 2.8 Ma, which may be incorrect due to a small number of analyzed grains.

At the Martel VD lithic tuff of rhyolites of presumed Turonian-Santonian age has been studied. The zircon grains separated from the sample AB-3/3 are represented by colorless idiomorphic crystals. Some of them of elongated prismatic and dipyramidal shape having elongation indices of 1.5–2.5, while other zircons are clasts of different size. The grain size varies from 50 to 120 μm. The CL images of zircons show concentric zonation for most grains and their clasts.

The obtained isotopic data are given in the Supplementary material in Table S1. The weighted average U–Pb age, based on 16 dating spots, of the sample AB-3/3 (Fig. 2*c*) from the middle part of the stratified section is 83.5 ± 1.0 Ma (Late Cretaceous: Campanian).

Petrographic description of rock units. *Martel VD.* In the geologic section of the Burelomny Stream (left tributary of the Belembe River, N 45°31′12″, E 136°43′) three rhythms of pyroclastic eruptions, expressed in the change of topographic elements of relief at the level of sampling, have been registered (AB-3/1–AB-3/3; AB-3/5–AB-3/8; AB-3/10–AB-3/15, from bottom to top). Crystal and lithic tuffs, and ignimbrites are distinguished. The volcanic rocks contain variable amounts of quartz, plagioclase, sanidine, rare pseudomorphs of chlorite after a primary biotite with a secondary magnetite, and pseudomorphs after pyroxene or amphibole. Each rhythm begins with extremely high-silica rocks, however, if the tuffs of the first and third rhythms are rich in quartz clasts, the initial eruptions of the second rhythm correlate with ignimbrites (Table 1). The latter are characterized not only by higher content of quartz but also by mostly quartziferous composition of the felsitic matrix. The rhythms end with eruptions of essentially rhyodacitic pyroclastic rocks enriched with mafic minerals and magnetite. The petrographic characteristics of pyroclastic rocks do not show the transition sequence that could be connected to the quartz fractionation, which is a factor explaining the contrast of composition variations in silica saturation. The high-silica volcanic rocks do not bear the marks of the superimposed silicification and fit naturally into the composition variations of the rock diversity.

South Yakut VD. The South Yakut VD volcanic rocks (N 44°17′10″, E 135°17′59″) are represented mostly by quartz-free rhyolites and ignimbrites, quartz rich lithic and lapilli-tuffs, and lapillistones. The rocks contain variable amounts of quartz, plagioclase, sanidine, rare pseudomorphs of chlorite after a primary biotite with a secondary magnetite. Tuffs and ignimbrites, though containing variable amounts of xenoliths, have statistically stable petrographic characteristics and are determined by the variations in their own mineral clasts; they do not bear the marks of the superimposed silicification or other secondary process.

Major and trace elements. The volcanic units of the South Yakut and Martel VD are rhyodacites, rhyolites and trachyrhyolites in composition (Table 1; Fig. 3*a*) and vary in silica contents (SiO_2 from 70.1 to 82.1 wt.%). They are characterized by normal and increased alkalinity of sodium-potassium rock types (K_2O from 1.6 to 8.0 wt.%, and Na_2O from 1.9 to 5.5 wt.%). The content of Al_2O_3 varies from 9.1 to 15.2 wt.%, which, together with the contents of alkali, characterizes them as metaluminous and peraluminous, less frequently as peralkaline (A/NK = 0.84–1.38, A/CNK = 0.80–1.33) (Table 1; Fig. 3*b*). The high concentrations of Al_2O_3 are typical of rhyodacites relatively rich in CaO, Eu, Sr, Ba. All samples have a high $FeO_{tot}/(FeO_{tot} + MgO)$ ratio varying from 0.86 to 0.98, which is similar to ferroan rocks according to (Frost et al., 2001) (Fig. 3*c*), and are characterized by low concentrations of MnO (0.01–0.11 wt.%), MgO (0.02–0.52 wt.%), CaO (0.05–0.78 wt.%), TiO_2 (0.07–0.31 wt.%) and P_2O_5 (<0.06 wt.%). All rocks exhibit wide concentration range of the LIL elements, and enrichment of HFSE (Zr, Nb, Ga and Y) and REE (except for Eu). As seen in the chondrite normalized rare earth element patterns, compositions of rocks have similar REE spectra showing an insignificant enrichment with LREE/HREE (3.5–10.5) at low values of the $(La/Yb)_N$ ratios (0.9 and 2.2–10.6) and negative Eu anomaly (Eu/Eu* = 0.1–0.6) (Fig. 3*h*). The total REE content varies from 38 to 193 ppm (Table 1). As seen in the primitive mantle-normalized trace element diagram, the rocks show negative Ba, Sr and Ti anomalies and positive K, Th, U, Pb, and also partially positive Ce, Zr and Hf anomalies (Fig. 3*g*), i.e., they demonstrate characteristics typical of geochemical *A*-type igneous rocks (Eby, 1990). Their position in the discriminant diagrams indicates the same (Whalen et al., 1987; Frost et al., 2001; Dall'Agnol and Olivera, 2007; Grebennikov, 2014) (Fig. 3*d–f*).

DISCUSSION

Causes of the geochemical specifics of volcanic rocks. The analysis of the geochemical composition of pyroclastic units of the studied objects has revealed similar cyclicity for

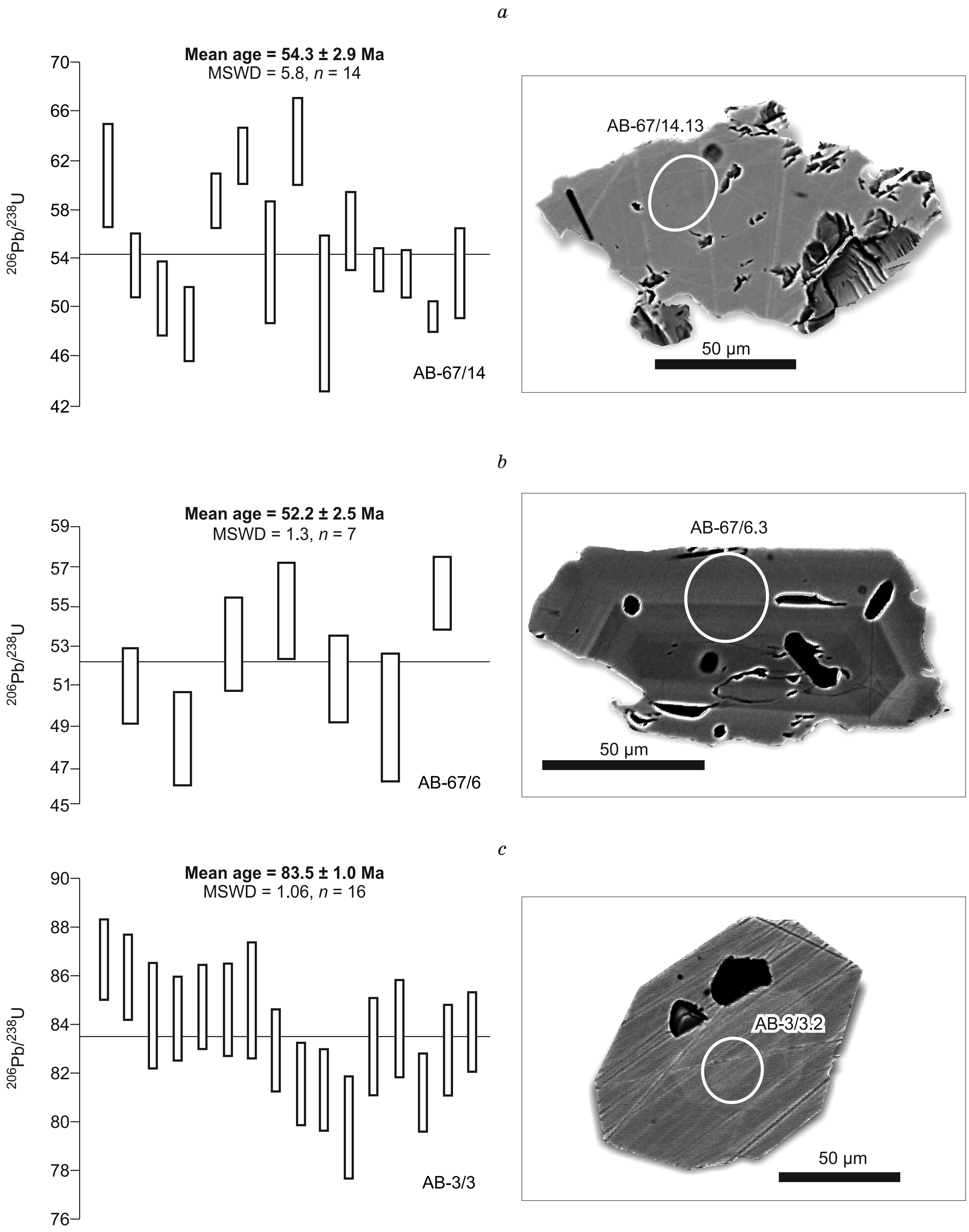

Fig. 2. Results of the LA-ICP-MS dating of the representative samples.

the ignimbrite eruptions of the Sikhote-Alin (Grebennikov and Maksimov, 2006). At the Martel VD we have distinguished three consecutive eruption rhythms expressed in the change of the chemical composition of each rock member of rhythm, starting from rhyolitic (up to 81 wt.% SiO_2) at the base to rhyodacitic (up to 70 wt.% SiO_2) at the upper parts of the Campanian volcanic formations (AB-3/1–AB-3/3; AB-3/5-AB-3/8; AB-3/10–AB-3/15, see Table 1). The obtained data allows us to assume that the first portions of ignimbrite-forming acidic melt, which were coming through

Table 1. Whole-rock geochemical compositions of the volcanic rocks

Component	AB-67	AB-67/1	AB-67/2	AB-67/3	AB-67/6	AB-67/11	AB-67/12	AB-67/14	AB-67/9	AB-3/1	AB-3/2	AB-3/3	AB-3/5	AB-3/6	AB-3/8	AB-3/10	AB-3/13	AB-3/15
	1	2	3	4	5	6	7	8	9	10	11	12	13	14	15	16	17	18
SiO_2	74.40	74.31	73.35	73.65	76.90	77.67	76.34	76.55	82.10	80.40	76.00	70.20	81.00	77.09	75.00	81.00	75.50	70.10
TiO_2	0.16	0.15	0.14	0.16	0.14	0.07	0.09	0.09	0.05	0.11	0.10	0.30	0.10	0.14	0.23	0.15	0.21	0.31
Al_2O_3	13.08	12.88	12.93	13.19	11.41	11.41	12.01	11.04	9.07	9.10	13.00	15.20	8.33	11.40	12.84	9.60	12.30	14.50
Fe_2O_3	1.52	1.37	0.97	1.21	1.11	0.58	0.73	0.58	0.33	0.36	0.79	2.17	1.09	1.02	1.59	1.12	1.38	2.70
FeO	0.36	0.45	1.13	0.32	0.45	0.35	0.42	0.56	0.47	0.33	0.21	1.01	0.48	0.49	0.53	0.35	0.68	0.67
MnO	0.05	0.05	0.06	0.04	0.03	0.02	0.01	0.01	0.01	0.01	0.00	0.06	0.03	0.00	0.02	0.02	0.02	0.04
MgO	0.11	0.08	0.09	0.10	0.05	0.03	0.05	0.02	0.02	0.05	0.05	0.52	0.11	0.04	0.10	0.05	0.17	0.50
CaO	0.18	0.22	0.68	0.16	0.10	0.10	0.08	0.20	0.06	0.30	0.55	0.89	0.07	0.60	0.27	0.07	0.50	0.78
Na_2O	5.54	3.78	4.40	3.97	3.61	3.25	3.59	1.97	3.10	4.25	3.67	4.54	2.10	5.23	3.29	2.80	2.20	4.70
K_2O	2.89	5.15	4.93	5.31	5.21	5.27	5.16	8.00	3.74	3.52	4.42	3.21	3.95	2.24	4.50	3.80	4.92	3.60
P_2O_5	0.01	0.01	0.01	0.02	0.03	0.00	0.00	0.00	0.00	0.01	0.01	0.05	0.00	0.00	0.03	0.00	0.02	0.06
H_2O^-	0.25	0.30	0.07	0.36	0.20	0.20	0.25	0.07	0.03	0.10	0.09	0.16	0.20	0.16	0.10	0.08	0.15	0.11
LOI	1.25	0.72	0.88	1.24	0.78	0.51	0.80	0.54	0.57	1.08	0.79	1.34	2.27	1.17	1.30	0.75	1.54	1.60
Σ	99.81	99.46	99.63	99.75	100.01	99.47	99.52	99.63	99.55	99.62	99.68	99.65	99.73	99.58	99.80	99.79	99.59	99.67
F	51	85	643	104	64	172	186	61	48	122	114	331	254	172	260	114	184	403
Zn	50.02	46.32	57.57	33.81	26.54	63.42	60.37	51.07	17.09	18.82	21.20	66.89	93.84	52.14	44.79	6.02	20.42	33.45
Ga	18.26	18.60	20.66	18.47	15.21	18.54	23.33	23.37	10.68	14.82	15.49	18.28	30.29	18.58	20.37	10.52	13.40	17.59
Rb	101.0	179.7	188.9	176.9	141.2	218.7	214.5	192.1	110.4	162.89	202.98	120.33	240.02	62.46	165.80	101.75	177.83	120.53
Sr	119.12	85.47	85.42	94.47	64.07	21.22	22.93	36.33	26.89	88.22	127.27	278.31	88.96	90.29	153.52	86.75	132.27	363.87
Y	24.97	24.54	37.03	33.00	27.81	42.58	35.00	19.83	33.67	10.38	25.13	25.84	36.82	20.09	17.85	8.69	19.90	31.22
Zr	179.2	193.9	203.5	190.8	164.4	136.7	143.8	180.4	105.9	124.73	108.14	276.12	171.16	217.47	187.08	106.05	148.24	244.24
Nb	12.61	12.97	13.49	12.51	17.94	21.15	21.34	16.52	16.52	18.45	21.17	11.54	14.78	12.99	8.83	5.48	9.22	12.70
Sn	4.06	4.31	4.02	2.98	1.04	4.84	5.54	5.55	3.85	2.50	3.88	1.95	3.84	3.73	1.21	4.61	4.31	2.31
Cs	2.80	3.32	3.52	3.54	2.23	4.59	4.60	1.10	2.38	14.79	4.52	3.94	16.81	3.82	14.57	4.32	4.38	2.09
Ba	640.24	798.74	786.3	832.7	936.4	225.4	188.6	598.3	297.1	353.79	186.02	917.95	616.68	282.75	1173.07	578.95	1075.25	890.97
La	16.38	21.82	39.74	40.01	9.39	15.86	12.95	33.41	4.32	3.53	19.04	34.67	28.61	29.80	15.56	14.78	16.83	31.42
Ce	47.08	66.63	78.83	63.63	61.68	62.13	53.18	73.93	11.51	21.14	45.11	76.78	66.73	64.88	41.76	30.18	37.12	67.93
Pr	3.73	5.67	9.29	8.54	3.03	4.19	3.52	7.83	1.50	1.01	5.24	8.68	7.84	7.03	4.84	3.22	4.30	8.29
Nd	12.98	18.24	33.21	30.53	12.99	15.47	13.45	27.84	5.22	3.01	18.49	33.17	30.87	26.46	19.99	11.17	17.63	30.44
Sm	3.16	4.82	7.69	6.25	3.97	4.76	3.75	5.95	2.14	0.85	4.80	6.83	6.56	4.24	3.92	1.83	3.90	5.97
Eu	0.36	0.48	0.90	0.74	0.44	0.14	0.15	0.62	0.11	0.10	0.29	1.23	0.75	0.18	0.95	0.38	0.79	1.39
Gd	2.75	3.27	5.80	5.06	3.34	4.72	3.23	4.02	2.76	1.15	3.90	5.84	6.30	3.86	3.73	1.67	3.91	6.26
Tb	0.52	0.59	1.01	0.92	0.72	1.04	0.71	0.70	0.71	0.24	0.73	0.86	1.13	0.55	0.61	0.25	0.66	0.92
Dy	4.47	4.77	6.77	5.65	4.87	8.13	5.61	4.80	5.66	1.87	4.86	5.32	7.54	3.66	3.65	1.40	3.60	5.30
Ho	0.91	0.85	1.20	1.02	0.93	1.48	1.27	0.86	1.05	0.43	1.09	1.19	1.53	0.86	0.81	0.32	0.78	1.09
Er	3.18	2.91	3.86	3.49	3.31	4.70	4.36	2.57	3.72	1.72	3.35	3.61	4.80	2.73	2.42	0.87	2.13	3.25

Tm	0.46	0.49	0.52	0.50	0.49	0.69	0.65	0.42	0.59	0.29	0.53	0.47	0.70	0.40	0.31	0.19	0.31	0.49
Yb	3.07	3.18	3.62	2.95	2.85	3.84	3.89	2.15	3.26	2.54	3.59	3.51	4.40	2.76	2.10	0.94	1.78	2.92
Lu	0.50	0.54	0.57	0.53	0.51	0.63	0.59	0.38	0.60	0.32	0.54	0.54	0.69	0.46	0.36	0.20	0.30	0.48
Hf	5.31	5.84	5.46	5.53	5.62	5.33	5.83	6.24	4.47	3.28	3.80	5.93	5.11	5.07	4.02	2.12	3.01	4.47
Ta	1.00	1.17	1.35	1.14	1.05	1.39	1.42	1.29	1.07	2.13	2.49	1.16	1.46	1.29	0.72	0.74	1.90	1.23
Pb	23.47	24.14	24.85	23.04	11.10	36.36	26.24	29.20	15.49	7.01	24.13	17.12	29.91	12.88	12.37	9.57	11.85	16.64
Th	17.30	17.63	18.51	18.46	12.24	17.11	17.60	15.92	11.60	14.32	25.57	11.85	13.94	12.58	5.79	7.49	14.56	12.71
U	3.68	3.63	3.79	3.87	2.29	4.09	3.88	3.32	2.53	2.93	6.22	2.48	3.03	2.70	2.60	1.31	2.89	2.52
ΣREE	99.55	134.24	193.01	169.80	108.50	127.78	107.31	165.46	43.16	38.19	111.55	182.68	168.46	147.87	101.00	67.39	94.03	166.16
LREE/HREE	5.27	7.09	7.27	7.44	5.38	4.06	4.28	9.41	1.35	3.46	5.00	7.56	5.22	8.67	6.22	10.54	5.98	7.03
$(La/Yb)_N$	3.59	4.63	7.41	9.15	2.22	2.78	2.24	10.49	0.89	0.94	3.58	6.66	4.38	7.29	4.99	10.65	6.36	7.26
Eu/Eu*	0.37	0.37	0.41	0.40	0.37	0.09	0.13	0.39	0.13	0.308	0.2	0.59	0.36	0.14	0.76	0.656	0.619	0.69
T_{Zr}, °C	805	815	803	811	794	784	788	794	765	751	765	851	811	812	820	769	805	830

Note: 1–9, volcanic rock compositions of South Yakut VD: lithic tuff (2, 4); crystal tuff (5, 6–7); ignimbrite (1, 3); lava (8); spherulite (9); 10–18, volcanic rock compositions of Martel VD: crystal tuff (10, 14, 16, 18); lithic tuff (12, 15); ignimbrite (11, 13, 17).
T_{ZR}(°C) = [12,900/(2.95 + 0.85 × M + ln$D^{Zr,\ zircon/melt}$)]-273, where $D^{Zr,\ zircon/melt}$ is Zr content ratio in zircon and the rock, M = (Na + K + 2 × Ca)/(Al × Si), (Watson and Harrison, 1983).
Eu/Eu* = $Eu_N/[(Sm_N) \times (Gd_N)]^{0.5}$.

the upper part of the exposed chamber, were consistent with the "high"-silica ignimbrites. The subsequent eruptions of the rhyodacitic melts were derived from the lower parts of the magma chamber. Thus, the "high" and "low"-silica diversities represent respectively more and less differentiated parts of one magma chamber that underwent the separation process of the primary magmatic melt.

Analogously, the early Eocene pyroclastic formations of the South Yakut VD are also characterized by the presence of the more welded "high"-silica ignimbrites, as well as by the "low"-silica tuffs. However, no clear interrelations between them can be observed due to the peculiarities of the pyroclastic unit complicated with multiple extrusive lava facies of the collapse caldera. Nonetheless, the geochemical characteristics of the volcanic rocks of these depressions, on the whole and specifically for the "high"- and "low"-silica differences, are practically identical (Table 1).

The principal chemical characteristics of the volcanic rocks of both VD are limited to the variations of SiO_2, K_2O, Na_2O and Al_2O_3 ratios. Their concentrations are expressed as CIPW Norm quantities of quartz (Q), albite (Ab) and K-feldspar (Or) in Table 2. The data analysis has shown that the bulk composition of rocks of the distinguished cycles (1 and 3 as most contrastingly expressed) of the ignimbrite eruptions of the Martel VD are settled along the line of equal compositions of the Or component with the enrichment of the residual ("low"-silica) Ab melts. Therewith, the earliest and most differentiated compositions of the volcanic rocks are more siliceous, while the residual ("low"-silica) compositions are more sodium. The latter are characterized by increasing alumina content (A/CNK) and total alkali concentration (Na_2O+K_2O) but decreasing FeO/(FeO+MgO) and A/CNK ratios (Table 2; Fig. 4).

Silica and alkali contents are similarly distributed (according to data of EPMA analyses) in the glasses of matrix and fiamme independently of ignimbrite type. In comparison with bulk compositions, fiamme are rich in Ab and Q components, thus characterizing the common Or→Ab→Q evolution of the primary melt, i.e., the accumulation of silica and sodium, and decrease in potassium in the most differentiated rocks. Therewith, glasses derived from the "high"-silica ignimbrites contain more sodium and are more siliceous, while glasses derived from the "low"-silica ones are more potassium. This probably indicates that fiamme are not liquation products but denote the residual melt (Grebennikov et al., 2012).

The bulk composition of rocks of the South Yakut VD are characterized by a more shortened differentiation trend (Table 2). The melt evolutions from "low" to "high"-silica differences follow the same geochemical patterns that are inherent to the volcanic rocks of the Martel VD. These features are further observed in the most fluidized parts of the magmatic melt, which currently takes the form of spherolitic rocks (Tables 1, 2; Fig. 4).

The behavior of some rare and trace elements from the rocks of the Martel VD is unusual, e.g., in "low-silica differ-

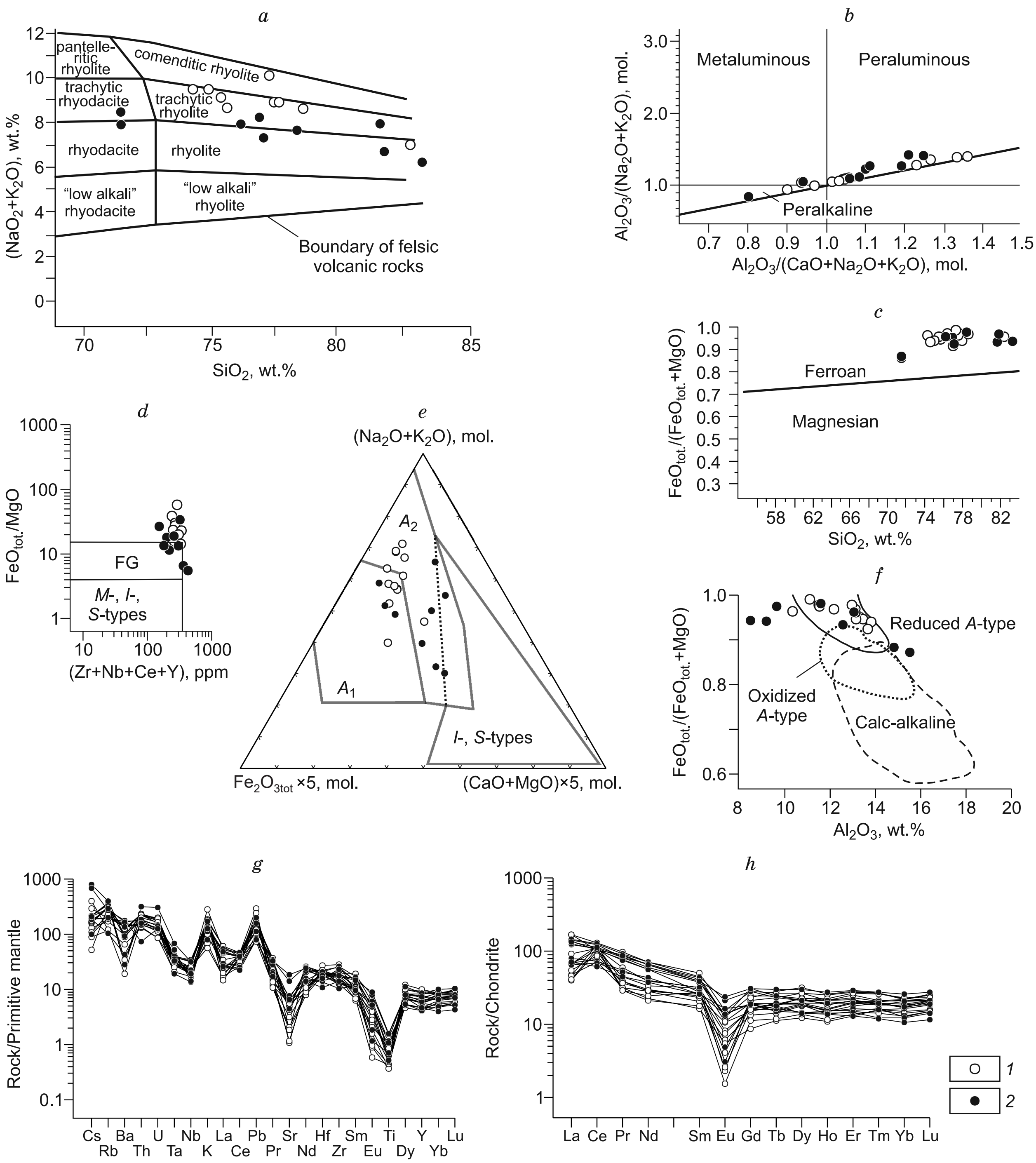

Fig. 3. Geochemical discriminant diagrams for the volcanic rocks of the South Yakut (*1*) and Martel (*2*) VD: *a*, TAS-diagram for the volcanic rocks (Bogatikov et al., 2008, 2009); *b*, A/NK ($Al_2O_3/Na_2O + K_2O$) vs. A/CNK ($Al_2O_3/CaO + Na_2O + K_2O$, all in molar quantities) diagram of Shand's index (Maniar and Piccoli, 1989); *c*, $FeO_{tot}/(FeO_{tot}+MgO)$ vs. SiO_2 (in wt.%) diagram showing the boundary between ferroan and magnesian silicic rocks and fields for *A*-, *S*-, and *I*-type rocks; the Fe-number line is defined as $FeO/(FeO + MgO) = 0.446 + 0.0046 \times SiO_2$ (Frost et al., 2001); *d*, (Zr + Nb + Ce + Y) – FeO_{tot}/MgO, discrimination diagram for *A*-type granites showing fields for fractionated felsic granites (FG) and non-fractioned *M*-, *I*-, and *S*-type granites (Whalen et al., 1987); *e*, (Na_2O+K_2O) – $Fe_2O_{3tot} \times 5$ – $(CaO + MgO) \times 5$, in molar quantities (Grebennikov, 2014); *f*, $FeO_{tot}/(FeO_{tot} + MgO)$ – Al_2O_3 (wt.%), with fields of "oxidized and reduced" *A*-type granites (Dall'Agnol and Olivera, 2007); *g*, composition of primitive mantle normalized rocks (McDonough and Sun, 1995); *h*, composition of chondrite normalized rocks (Sun and McDonough, 1989).

Table 2. Main petrochemical indicators for the representative volcanic rocks of the South Yakut and Martel VD

	SiO_2 (wt.%)	Fe_{tot}/Mg	Al_2O_3 (mol.)	Na_2O (mol.)	K_2O (mol.)	NK/A	A/CNK	CIWP Norm data (%)	Zr/Hf	Nb/Ta	Rb/Sr
South Yakut VD											
Spherulite	82.10	50.00	89.89	50.55	40.13	1.01	0.98	Q(50)>Ab(26)>Or(22)	23.71	15.41	4.11
"high"-silica rocks	76.90	32.50	113.02	58.82	55.85	1.01	0.97	Q(36)>Or(31)>Ab(30)	29.25	17.13	2.20
	77.67	29.70	113.34	53.07	56.67	0.97	1.02	Q(39)>Or(32)>Ab(28)	25.67	15.19	10.31
	76.34	24.68	119.65	58.73	55.58	0.96	1.03	Q(36)>Or(31)>Ab(31)	24.69	15.03	9.35
"low"-silica rocks	73.65	14.80	131.83	65.30	57.44	0.93	1.05	Ab(34)>Or(32)>Q(30)	34.53	10.99	1.87
	74.31	21.58	128.36	61.93	55.51	0.91	1.06	Ab(32)≥Q(32)>Or(31)	33.20	11.13	2.10
	73.35	24.37	128.54	71.84	53.05	0.97	0.94	Ab(38)>Or(30)>Q(28)	37.30	9.96	2.21
Martel VD											
1st-cycle	80.40	13.80	90.68	69.64	37.96	1.19	0.80	Q(47)>Ab(28)>Or(21)	38.07	8.65	1.85
	70.20	6.12	151.92	74.61	34.72	0.72	1.21	Ab(39)>Q(29)>Or(19)	46.54	9.93	0.43
2nd-cycle	81.00	14.27	84.02	34.83	43.11	0.93	1.06	Q(55)>Or(24)>Ab(18)	33.46	10.14	2.69
	75.00	21.20	128.00	53.93	48.55	0.80	1.19	Q(38)>Ab(28)>Or(27)	46.52	12.25	1.08
3rd-cycle	81.00	29.40	95.16	45.64	40.76	0.91	1.09	Q(50)>Ab(24)>Or(23)	49.91	7.41	1.17
	70.10	6.74	145.20	77.39	39.01	0.80	1.11	Ab(41)>Q(27)>Or(22)	54.61	10.33	0.33

Note: Q, quartz; Ab, albite; Or, orthoclase (sanidine).

ences" we register relatively high values of Ba, Sr and Eu, the total quantity of REE and values of Zr/Hf, Nb/Ta increase, while Rb/Sr values decrease (Table 1). The same tendency is mainly observed in the rocks of the South Yakut VD (Fig. 5). The low values of Ba, Sr and Eu are frequently associated with the fractionation of plagioclase under regular processes of the magmatic differentiation. However, in case of such supercooled high-viscosity melt systems with a fluoride fluid component, the depleted concentration of Eu can be explained rather by the influence of an acidic magmatic fluid and removal of divalent cations (Eu, Ba, Sr) from the melt, than by the plagioclase effect (Zharikov, 1996). This is confirmed by the negative correlation of Eu/Eu* (Table 1). The regular fractionation of plagioclase cannot account for such a high degree of Eu anomaly (Irber, 1999; Jahn et al., 2001).

We believe that the typical variations of the chemical composition of rocks from the studied VD should be related to the enrichment of the upper part of the magma chamber with fluid components, and to the respective redistribution of the mobile elements patterned after the fluid-magmatic differentiation. The eruptive alternation of conventionally "low"-silica and "high"-silica rhyolites, differing in their geochemical and mineralogical composition, is determined by the periodically occurring zonation of the magma chamber resulting from the generation of the fluidized melt in the head of the column. The presented data permit to assume that cyclic changes in composition of ignimbrite melts are essentially caused by the processes of the fluid-silicate cluster differentiation of the initially homogeneous melt (Bezmen, 2001; Bezmen and Gorbachev, 2014). The experimental studies demonstrated that under pressure the fluid phase (H, O, C) with a mole fraction of H constituted 0.03 in presence of F and P, the super-liquidus differentiation developed in granite melts followed by the separation of the SiO_2 rich melt (Bezmen et al., 1999, 2005). On the whole, these composition variations are consistent with the experiment results obtained for the high fluoride leucogranite systems. According to Manning (1981) the F enrichment of the system moves the eutectic and cotectic proportion of the acidic melt to a less silica saturated field enriched in alkali, therefore confirming the natural phenomenon most contrastingly manifested in the rocks of the Martel VD, where a consecutive, repeatedly alternating eruption of high- and moderate-silica differences is registered. Concurrently, the experimental works (Devyatova et al., 2007) point out that the F content in igneous rocks can be rather low, but it is not consistent with the actual content in the respective melts. Even a small quantity of F significantly influences the mineral equilibria and greatly mobilizes a whole series of rare metals. In quartz-normative rocks depleted in alkali the concentration of F content grow in high-silica melts (up to 12–14 at.%). The existence of such a melt is interpreted as a prototype of a quartzolite (or silexite) melt that used to be formed at the final stages of the magmatic evolution. The moderate concentration of F in the studied rhyolites reflects not its true initial content but the depletion in divalent strong cations (first of all, of Ca) of this geochemical rock type. This is confirmed by the correlation of CaO and F concentrations (Table 1). At the final stage fluorine is redistributed entirely to the fluid phase impoverishing the melt as the temperature falls and F concentrates in the fluorine-containing minerals (Aksyuk, 2002). It is even more difficult to assess the hydrogen's part in the evolution of acidic silicate melts because of its extremely high volatility. Its indirect contribution consists in the abundance of supercooled liquids (glasses), enormous percent of pyroclastic fragments, the anomalous ferruginous content of Fe–Mg silicates, domination of

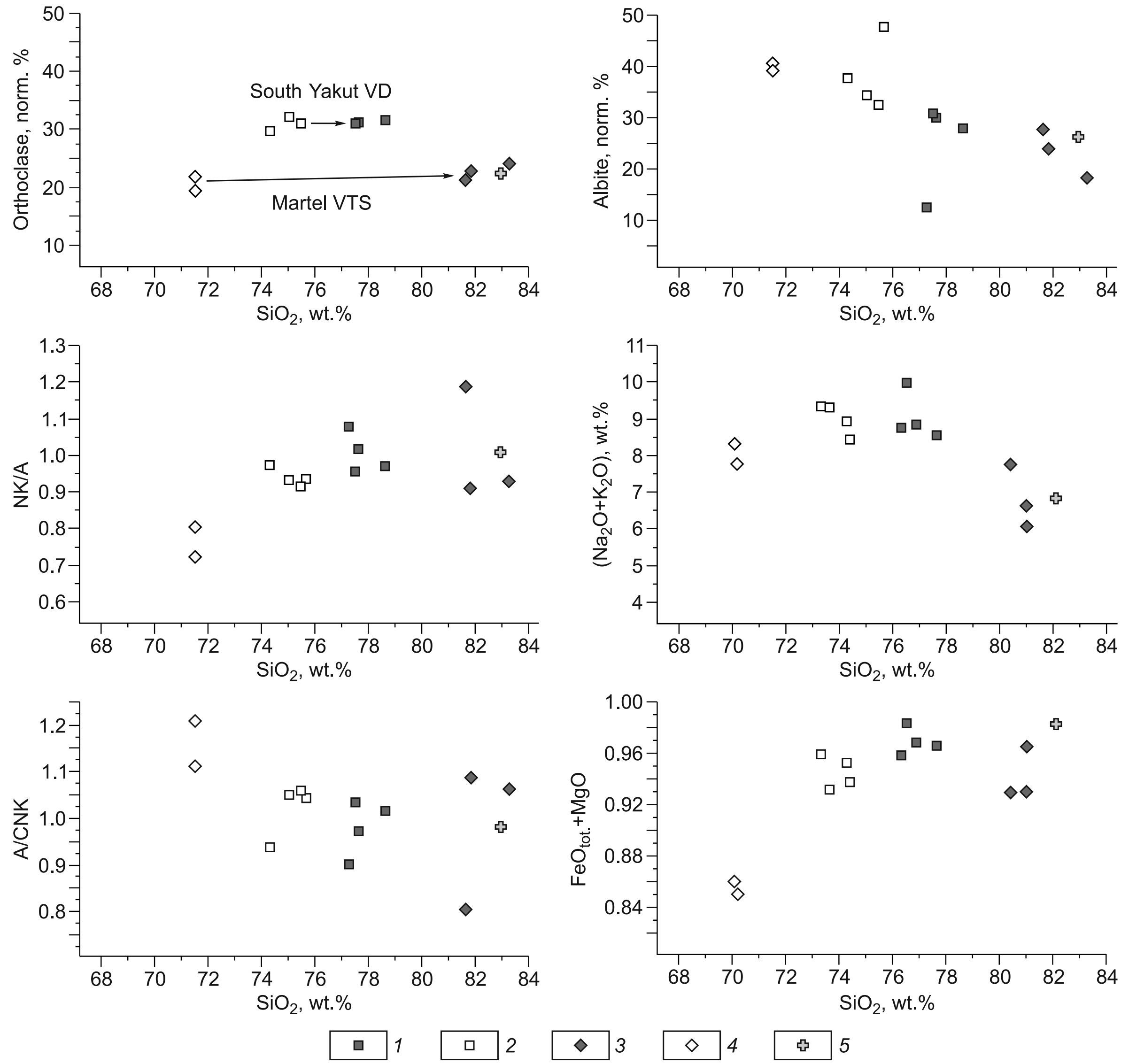

Fig. 4. Binary diagrams for the most contrasting types of "low"- and "high"-silica rocks of the South Yakut (1–2) and Martel (3–4) VD, respectively; spherulite composition from the rhyolitic lava at the South Yakut VD (5).

ilmenite and rare presence of magnetite, and, finally, the occurrence of silicate–metallic spherules that contain native iron in the volcanic rocks of the studied VD (Grebennikov, 2011; Grebennikov et al., 2012). The process of formation of significant volumes of the non quenching glassy phase can reflect an «oxygen expense» to neutralize the reduced (hydrogen) fluid, the destruction of structural forms of silicates, and in fact the melt amorphization (Pospelov, 1973).

Apparently the differentiation character of acidic melts in a shallow setting with the enrichment of the upper part of the magma chamber with fluid components and the respective redistribution of the mobile micro- and macro-components patterned after the fluid-magmatic differentiation could be determined by the openness of magma chambers to the outside environment (Popov and Grebennikov, 1997).

The rocks of the South Yakut VD is represented mainly by the extrusive lava (spherolitic rhyolites) and ignimbrite units. The felsic magma rich in gases was forced out through the conduits. Coming out to the day surface, the emitted in a short time gases transformed magma in a moving foam. Spreading around the conduits, this moving foam created volcanic glasses or spherolitic rocks. Apparently this phenomenon took place during the formation of the edifices of felsic rocks under the conditions of an "open" system.

The cyclic alternation of conventionally "low"-silica and "high"-silica pyroclastic rhyolites with their intermediate counterparts of the Martel VD, differing in petrogeochemical and mineralogical characteristics, reflects the processes of the fluid differentiation of silicic melt under quasistatic (closed) conditions.

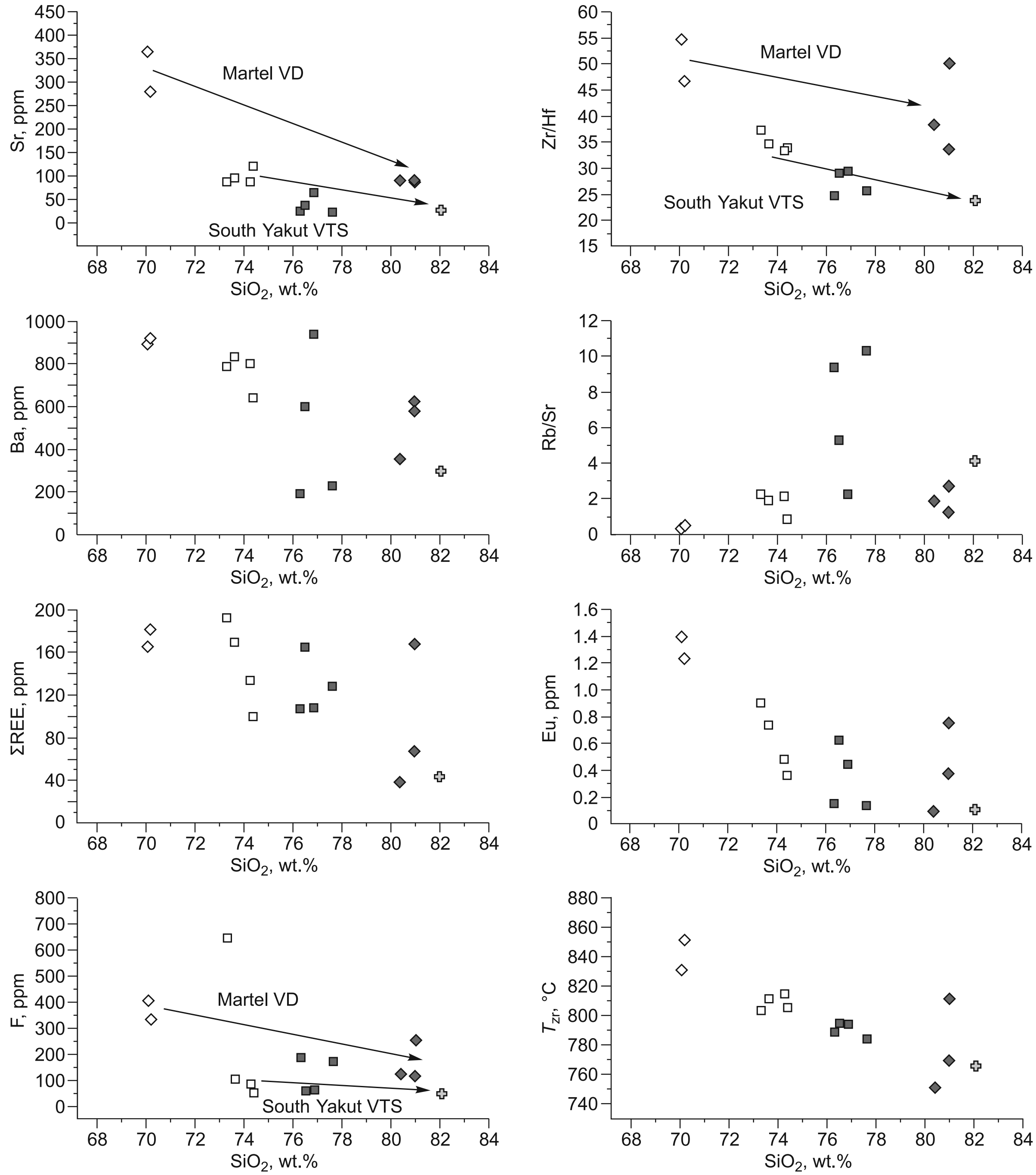

Fig. 5. Variation diagram of the key elements and ratios for the most contrasting types of "low"– and "high"-silica rocks of the South Yakut (1–2) and Martel (3–4) VD respectively; spherulite composition from the rhyolitic lava at the South Yakut VD (5). For notation see Fig. 4.

Thermal regime of zircon crystallization. Zircon, the composition, structure and textural features of which reflect the rock formation conditions, is an informative accessory mineral that can be used as a geothermometer to assess the thermal regime.

The review of literature on magmatic rocks, having U–Pb zircon dating and data on the elemental composition, revealed two groups of intrusives with temperatures of 772 ºC and 831 ºC. The low-temperature ("cold") granitoids suggest a melting mechanism whose temperature of magma could not surpass 800 ºC (Chappell et al., 1998; Miller et al., 2003). Their formation occurs mainly under the conditions of decompression melting with a little influence of the deep thermal source caused by the upwelling of the magma in crystal-poor state. During the interaction with mafic magma the temperature can increase but not necessarily. All "cold" granites are drawn to the areas of the Earth's crust growth. Simultaneously, the formation of "hot" granites at a temperature of >800 ºC requires heat inflow, which accounts for the injection of mafic magmas. These temperatures correlate with the modern models of silicic magma formation (dehydration melting in the Earth's crust; fractionation of the mantle-derived melts with or without the crustal contamination). Most "hot" granites, tectonic settings of which were established, intruded transtensionally.

The temperature of Zr saturation (Watson and Harrison, 1983) calculated for the volcanic rocks of the South Yakut and Martel VD is 779–832 ºC and 751–830 ºC, given the average values of 802 ºC and 813 ºC respectively (Table 1). The obtained data should be regarded as minimum points of the liquidus temperature because the inherited zircon cores are missing. This suggests that the studied *A*-type rocks formed at relatively high temperatures. The lower temperatures of the crystallization of "high"-silica rhyolitic magmas at both the South Yakut and Martel VD allow for the existence of temperature zoning in peripheral magma chambers (Table 1). On the one hand this implies a heat inflow from the deep basaltic chamber, on the other hand the enrichment of the head part of the magma column with a fluid component. It is known that fluid components, possessing high solubility in melts (such as F, H_2O, etc.), decrease considerably the temperature of the melt crystallization and contribute to density reduction, thus accounting for gravitational instability and fluid accumulation in the upper part of the magma chamber.

Geological and structural criteria of magma generation. The modern data on stratigraphy, metamorphism, and geology of the Far Eastern part of the Pacific margin (Faure and Natal'in, 1992; Nokleberg et al., 2000; Golozubov, 2006; Kemkin, 2006; Khanchuk, 2006; Parfenov et al., 2010; Utkin, 2013; Jahn et al., 2015) permitted to identify the main features of the region's development. Its Mesozoic and Cenozoic history can reflect the alternating episodes of the settings of subduction and California type transform margin (Khanchuk and Ivanov, 1999; Khanchuk and Kemkin, 2003; Martynov et al., 2017; Khanchuk et al., 2019).

Within the limits of the continental margin of the Asian continent the Eastern Asia Volcanic Belt, including the East Sikhote-Alin branch (ESAVB), unique in its extent formed in the Upper Cretaceous. At the initial stage its magmatic history is characterized by eruptions of basalts and andesites of the Sinancha complex (Cenomanian), later by eruptions of large masses of tuffs and ignimbrites of acidic composition of the Primorye series (Turonian–Santonian) and at the final stage it is characterized by the formation of andesites of the Samarga, and Dorofeevka (Maastrichtian) and almost simultaneous dacites, rhyodacites of the Siyanovka volcanic complexes (Khanchuk, 2006). The Turonian–Santonian felsic ignimbrites form the bulk of the ESAVB and are characterized by a homogeneous composition, high predominance of the welded tuffs and rhyolitic ignimbrites, and gigantic (up to 1500 m) thickness. The plant fragments found in the volcanogenic sedimentary rocks allow to determine two ages – Turonian–Coniacian and Coniacian–Santonian (Mikhailov, 1989). Concurrently the U–Pb dating showed a younger age of the intrusive bodies that intruded effusive edifices – 82.7–70.4 Ma (Jahn et al., 2015; Tsutsumi et al., 2016). Their magnesian-ferruginous, calcareous and calc-alkaline compositions correspond to high-alumina acidic magmas of *I*- and *S*-type. The formation of such melts is explained by the partial melting of metasedimentary and metaigneous rocks in a relatively oxidizing environment with water fluids typical for the volcanism of the suprasubduction geodynamic settings.

The initial development stages of the Cenozoic volcanism relate to the formation of the Paleocene–Eocene igneous complex. Its distinctive feature is the close spatial relationship with large sub-latitudinal volcanic depressions superimposed on the heterogeneous structures of the continental margin, including the Upper Cretaceous ESAVB. The volcanic rocks of the complex differ greatly in their composition from Turonian–Campanian felsic rocks and correspond to the geochemical *A*-type (Grebennikov and Popov, 2014). The volcanic rocks' age determined by precursors using the Rb-Sr and U–Pb methods is 59.7–53.0 Ma (Popov and Grebennikov, 2001; Grebennikov and Maksimov, 2006; Alenicheva and Sakhno, 2008; Sakhno et al., 2010; Jahn et al., 2015; Pavlyutkin et al., 2016; Tang et al., 2016; Sakhno and Kovalenko, 2018). At this time the region's tectonic development was characterized by several hundred kilometers long displacements along the edge of the continental plate (Utkin, 1980), and pull-apart basin formation followed by the development of specific magmatic complexes including the *A*-type (Khanchuk et al., 2019). The occurrence of the low-magnesian *A*-type igneous rocks, as opposed to the calc-alkaline high-alumina and/or medium-magnesian complexes (*I-S*-type), is possible only in the zones of the lithospheric extension due to the interaction between the sublithosphere mantle and material of the continental crust (e.g., Bonin, 2007; Grebennikov and Maksimov, 2006; Grebennikov, 2014; Grebennikov and Popov, 2014; Grebennikov et al., 2016; Khanchuk et al., 2019).

According to the reconstructions (Engebretson et al., 1985), the motion vector of the Pacific plate changed from 338° NW to 294° NW at c. 85 Ma, and at c. 53 Ma it changed back from NW to almost submeridional (from 314° NW to 358° NW), the deviation being the same 44° (Fig. 6). It is unlikely that these transformations were momentary. Nonetheless, the indicated geodynamic boundaries fully coincide with the age-data of both *A*-type rocks presented in this study and in those published earlier.

We suggest two alternative geodynamic models: 1) successive enhancement of shear impulses with complementary growth of hardness of the extensional component and, con-

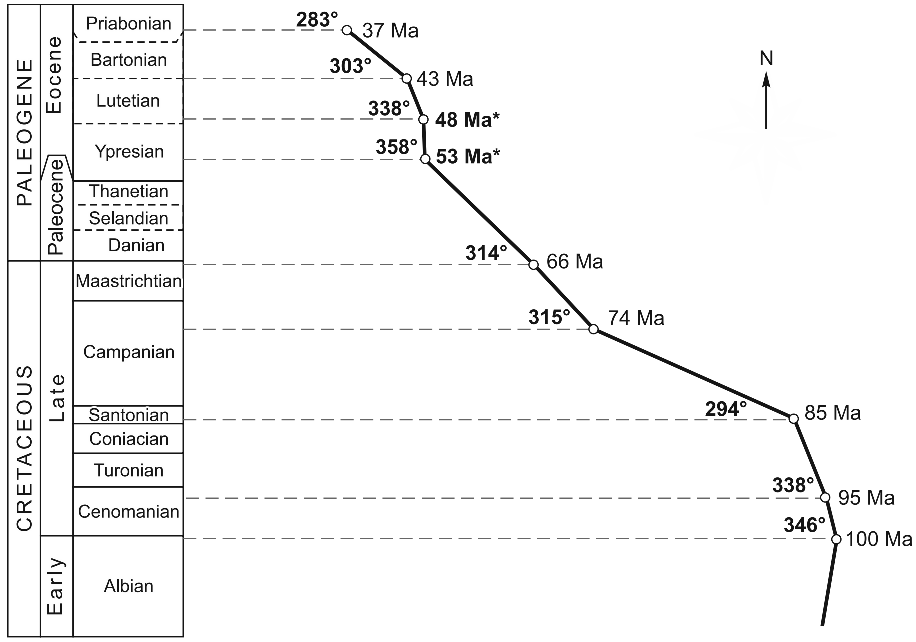

Fig. 6. Stratigraphic scale and Pacific plate motion vector. Bold, insufficiently reliable data (Engebretson et al., 1985, p. 41).

sequently, depth of magma-fluid control; and 2) sudden change of the motion vector of the Pacific plate in respect to the continental plate, which resulted in stagnation and destruction of the slab with a possible discontinuity (slab-window, slab tear) and injection of asthenospheric (subslab) mantle. The involvement of the mantle high-temperature reduced fluids (almost anhydrous, of mainly H_2 and CH_4 composition) accounted for the partial melting of the crustal material followed by the formation of melts as sources of igneous *A*-type rocks. The origin of this type of acidic melts relates to the penetration depth of the cracks in lithosphere conjugated with the shear dislocations (extensional systems), velocities (impulses) of their opening (that accounted for such depth), and to the permeability of the continental crust as well as to its degree of consolidation. Multiple publications have described in detail the kinematics of these dislocations (e.g., Utkin, 2005, Nevolin et al., 2014). However, magmatism of this "specific geochemical type" was not registered on the territory of the Albian-Cenomanian marginal continental orogenic belt (Sikhote-Alin) distinguished by A.I. Khanchuk and co-authors (2019), that represents a newly formed part of the continental lithosphere, which originated in the transform continental margin setting. On the whole the change in the geodynamic regime and conjugate magmatism tend to take place along all of the Eastern Asia Volcanic Belt but with a temporary displacement within some of its fragments, and occurrence of analogs to the *A*-type magmatites: Urak and Nitkan (Priokhotye region), Belouvalensk complexes (Chukotka region).

CONCLUSIONS

1) New isotopic-geochemical data for the volcanic rocks of the South Yakut and Martel VD indicate that they formed in the early Eocene (54.3 ± 2.9 Ma) and early Campanian (83.5 ± 1.0 Ma) respectively.

2) The calculated temperature T_{ZR}°C (800 ºC on average) allows for the initial melts being of high temperature, while the geochemical properties of volcanic rocks of these structures confirm the highly differentiated composition of magmas enriched with volatile components, and their belonging to the rocks of the geochemical *A*-type.

3) The compositional zoning of the derivatives of the peripheral magma chamber could be caused by the enrichment of the head part of the magma column with fluid components. These components practically led to the melt fluidization, replacement of calcareous and magnesium cation components with alkali-ferruginous components, increase in values of NK/A and Fe_{tot}/Mg, and decrease in melt temperature (T_{ZR}°C).

4) We identified the logical correlation between the formation of igneous rocks of the South Yakut and Martel VD and the large-scale Campanian and Paleocene–Eocene shear dislocations in the process of activation of the transform Pacific margin and evolution of the regional shear structure of the Sikhote-Alin. Furthermore, the development of the destructive structures and deep permeability of the continental crust followed. This caused the injection of subslab asthenospheric material and reduced (fluorine-hydrogen) fluid flows that accounted for the generation of the *A*-type melts from the crustal component.

We are grateful to V.G. Khomich (FEGI FEB RAS, Vladivostok), N.N. Kruk and O.M. Turkina (IGM SB RAS, Novosibirsk) and E.V. Sklyarov (IEC SB RAS, Irkutsk) for critical comments that significantly improved the manuscript.

This work was financially supported by the Russian Foundation for Basic Research (project No. 19-05-00100), as well as by the Russian Foundation for Basic Research and the State Foundation for Natural Sciences for China (project No. 19-55-53008).

REFERENCES

Aksyuk, A.M., 2002. Experimentally established geofluorimeters and the fluorine regime in granite-related fluids. Petrology 10 (6), 557–569.

Alenicheva, A.A., Sakhno, V.G., 2008. The U–Pb dating of extrusive-intrusive complexes in ore districts in the southern part of the Eastern Sikhote-Alin Volcanic Belt. Dokl. Earth Sci. 419 (2), 217–221, doi:10.1134/S1028334X08020062.

Bezmen, N.I., 2001. Superliquidus differentiation of fluid-bearing magmatic melts under reducing conditions as a possible mechanism of formation of layered massifs: experimental investigations. Petrology 9 (4), 345–361.

Bezmen, N.I., Gorbachev, P.N., 2014. Experimental investigations of superliquidus phase separation in phosphorus-rich melts of Li-F granite cupolas. Petrology 22 (6), 574–587, doi:10.1134/S0869591114060022.

Bezmen, N.I., Fed'kin, A.V., Zaraisky, G.P., 1999. Experimental study of phosphorus and fluorine influence on the super-liquidus differentiation of granite melts: preliminary data. Exp. Geosci. 8 (1), 49–53.

Bezmen, N.I., Zharikov, V.A., Kalinichev, A.G., Zevel'sky, V.O., 2005. Melting of alkali aluminosilicate systems under hydrogen-water fluid pressure, P_{tot} = 2 kbar. Petrology 13 (5), 407–426.

Black, Z.P., Kamo, S.Z., Allen, C.M., Davis, D.W., Aleinikoff, J.N., Valley, J.W., Mundil, R., Campbell, I.H., Korsch, R.J., Williams, I.S., Foudoulis, C., 2004. Improved $^{206}Pb/^{238}U$ microprobe geochronology by the monitoring of a trace-element-related matrix effect; SHRIMP, ID–TIMS, ELA–ICP–MS and oxygen isotope documentation for a series of zircon standards. Chem. Geol. 205, 115–140, doi:10.1016/j.chemgeo.2004.01.003.

Bogatikov, O.A., Petrov, O.V., Sharpenok, L.N. (Eds.), 2008. Petrographic Code of Russia. Magmatic, metamorphic, metasomatic, and impact formations [in Russian]. VSEGEI Press, St. Petersburg.

Bogatikov, O.A., Petrov, O.V., Morozov, A.F. (Eds.), 2009. Petrographic Code of Russia. Magmatic, metamorphic, metasomatic, and impact formations [in Russian]. VSEGEI Press, St. Petersburg.

Bonin, B., 2007. A-type granites and related rocks: evolution of a concept, problems and prospects. Lithos 97, 1–29, doi:10.1016/j.lithos.2006.12.007.

Bonin, B., Azzouni-Sekkal, A., Bussy, F., Ferrag, S., 1998. Alkali-calcic and alkaline post-orogenic (PO) granite magmatism: petrologic constraints and geodynamic settings. Lithos 45, 45–70, doi:10.1016/S0024-4937(98)00025-5.

Bykovskaya, E.V., Polevaya, N.I., Podgornaya, N.S., 1960. Absolute age of the Mesozoic-Cenozoic volcanogenic and intrusive rocks of the Olga-Tetyukhinsky District. Sovetskaya Geologiya, No. 5, 107–113.

Chappell, B.W., Bryant, C.J., Wyborn, D., White, A.J.R., Williams, I.S., 1998. High- and low-temperature I-type granites. Res. Geol. 48, 225–236, doi:10.1111/j.1751-3928.1998.tb00020.x.

Dall'Agnol, R., Olivera, D.C., 2007. Oxidized, magnetite-series, rapakivi-type granites of Carajas, Brasil: implications for classification and petrogenesis of A-type granites. Lithos 93, 215–233, doi:10.1016/j.lithos.2006.03.065.

Dall'Agnol, R., Frost, C.D., Rämö, O.T., 2012. IGCP project 510 "A-type granites and related rocks through time": project vita, results, and contribution to granite research. Lithos 151, 1–16, doi:10.1016/j.lithos.2012.08.003.

Devyatova, V.N., Gramenitskii, E.N., Shchekina, T.I., 2007. Phase relations in fluorine-bearing granite and nepheline syenite systems at 800 °C and 1 kbar. Petrology 15 (1), 19–34, doi: 10.1134/S086959110701002X.

Eby, G.N., 1990. The A-type granitoids: A review of their occurrence and chemical characteristics and speculations on their pedogenesis. Lithos 26, 115–134.

Engebretson, D., Cox, A., Gordon, R.G., 1985. Relative motions between oceanic and continental plates in the northern Pacific basin. Geol. Soc. Am. Spec. Pap. 206, 1–59.

Faure, M., Natal'in, B., 1992. The geodynamic evolution of the eastern Eurasian margin in Mesozoic times. Tectonophysics 208 (4), 397–411, doi:10.1016/0040-1951(92)90437-B.

Frost, B.R., Barnes, C.G., Collins, W.J., Arculus, R.J., Ellis, D.J., Frost, C.D., 2001. A geochemical classification for granitic rocks. J. Petrol. 42 (11), 2033–2048, doi:10.1093/petrology/42.11.2033.

Golozubov, V.V., 2006. Tectonics of the Jurassic and Lower Cretaceous Complexes of the Northwestern Framing of the Pacific Ocean [in Russian]. Dal'nauka, Vladivostok.

Grebennikov, A.V., 2011. Endogene spherules of Cretaceous-Paleogene Ignimbrite complexes of Yakut volcane-tectonic structure (Primorye). Zapiski Russkogo Mineralogicheskogo Obshestva, Vol. CXXXX (3), 56–68.

Grebennikov, A.V., 2014. *A*-type granites and related rocks: petrogenesis and classification. Russian Geology and Geophysics (Geologiya i Geofizika) 55 (9), 1074–1086 (1356–1373).

Grebennikov, A.V., Maksimov, S.O., 2006. Fayalite rhyolites and a zoned magma chamber of the Paleocene Yakutinsky volcanic depression in Primorye, Russia. J. Mineral. Petrol. Sci. 101 (2), 69–88.

Grebennikov, A.V., Popov, V.K., 2014. Petrogeochemical aspects of the Late Cretaceous and Paleogene ignimbrite volcanism of East Sikhote-Alin. Russ. J. Pac. Geol. 8 (1), 38–55, doi:10.1134/S1819714014010035.

Grebennikov, A.V., Shcheka, S.A., Karabtsov, A.A., 2012. Silicate–metallic spherules and the problem of the ignimbrite eruption mechanism: The Yakut volcanic depression. J. Volcanol. Seismolog. 6 (4), 211–229, doi:10.1134/S0742046312040021.

Grebennikov, A.V., Khanchuk, A.I., Gonevchuk, V.G., Kovalenko, S.V., 2016. Cretaceous and Paleogene granitoid suites of the Sikhote-Alin area (Far East Russia): geochemistry and tectonic implications. Lithos 261, 250–261, doi:10.1016/j.lithos.2015.12.020.

Irber, W., 1999. The lanthanide tetrad effect and its correlation with K/Rb, Eu/Eu*, Sr/Eu, Y/Ho and Zr/Hf of evolving peraluminous granite suites. Geochim. Cosmochim. Acta 63, 489–508, doi:10.1016/S0016-7037(99)00027-7.

Jahn, B.-M., Wu, F., Capdevila, R., Martineau, F., Zhao, Z., Wang, Y., 2001. Highly evolved juvenile granites with tetrad REE patterns: the Woduhe and Baerzhe granites from the Great Xing'an Mountains in NE China. Lithos 59, 171–198, doi:10.1016/S0024-4937(01)00066-4.

Jahn, B.-M., Valui, G., Kruk, N., Gonevchuk, V., Usuki, M., Wu, J.T.J., 2015. Emplacement ages, geochemical and Sr–Nd–Hf isotopic characterization of Mesozoic to early Cenozoic granitoids of the Sikhote-Alin Orogenic Belt, Russian Far East: crustal growth and regional tectonic evolution. J. Asian Earth Sci. 111, 872–918, doi:10.1016/j.jseaes.2015.08.012.

Kemkin, I.V., 2006. Geodynamic Evolution of the Sikhote-Alin and Sea of Japan Region in the Mesozoic [in Russian]. Nauka, Moscow.

Kemkin, I.V., Khanchuk, A.I., Kemkina, R.A., 2016. Accretionary prisms of the Sikhote-Alin Orogenic Belt: Composition, structure and significance for reconstruction of the geodynamic evolution of the eastern Asian margin. J. Geodyn. 102, 202–230, doi: 10.1016/j.jog.2016.10.002.

Khanchuk, A.I. (Ed.), 2006. Geodynamics, Magmatism and Metallogeny of the Russian East [in Russian]. Dal'nauka, Vladivostok.

Khanchuk, A.I., Ivanov, V.V., 1999. Meso-Cenosoic geodynamic settings and gold mineralization of the Russian Far East. Russian Geology and Geophysics (Geologiya i Geofizika) 40 (11), 1607–1617 (1635–1645).

Khanchuk, A.I., Kemkin, I.V., 2003. Geodynamic evolution of the Sea of Japan Region in the Mesozoic. Vestnik DVO RAN, No. 6, 99–116.

Khanchuk, A.I., Grebennikov, A.V., Ivanov, V.V., 2019. Albian–Cenomanian orogenic belt and igneous province of Pacific Asia. Russ. J. Pac. Geol. 13 (3), 187–219, doi:10.1134/S1819714019030035.

Kovalenko, A.P., Zhuravlev, V.N., Kovalenko, R.A., 1968. On bertrandite mineralization in young volcanogenic rocks. Geologiya Rudnykh Mestorozhdenii, No. 10 (5), 87–90.

Malinovsky, A.I., Filippov, A.N., Golozoubov, V.V., Simanenko, V.P., Markevich, V.S., 2002. Lower Cretaceous deposits of the Kema river area (Eastern Sikhote-Alin): sedimentary filling of a back-ark basin. Tikhookeanskaya Geologiya, No. 21 (1), 52–66.

Maniar, P.D., Piccoli, P.M., 1989. Tectonic discrimination of granitoids. Geol. Soc. Am. Bull. 101, 635–643.

Manning, D.A.C., 1981. The effect of fluorine on liquidus phase relationship in the system Qz-Ab-Or with excess water at 1 kb. Contrib. Mineral. Petrol. 76, 206–215, doi:10.1007/BF00371960.

Martynov, Yu.A., Khanchuk, A.I., Grebennikov, A.V., Chashchin, A.A., Popov, V.K., 2017. Late Mesozoic and Cenozoic volcanism of the East Sikhote-Alin area (Russian Far East): A new synthesis of geological and petrological data. Gondwana Res. 47, 358–371.

Matyunin, A.P., 1988. Magmatism of the Kavalerovsky and Verkhnearminskiy Tin-Bearing Areas, PhD. Thesis [in Russian]. DVGI DVO AN SSSR, Vladivostok.

McDonough, W.F., Sun, S.-S., 1995. The composition of the Earth. Chem. Geol. 120, 223–253, doi:10.1016/0009-2541(94)00140-4.

Mikhailov, V.A., 1989. Magmatism of Volcanotectonic Structures in the South of the East Sikhote-Alin Volcanic Belt [in Russian]. DVO AN SSSR, Vladivostok.

Miller, C.F., McDowell, S.M., Mapes, R.W., 2003. Hot and cold granites? Implications of zircon saturation temperatures and preservation of inheritance. Geology 31, 529–532.

Nazarenko, L.F., Bazhanov, V.A., 1989. The Geology of the Primorye. Part 1. The Stratigraphy [in Russian]. DVO AN SSSR, Vladivostok.

Nevolin, P.L., Utkin, V.P., Mitrokhin, A.N., Kasatkin, S.A., 2013. Role of latitudinal compression in the formation of Paleozoic intrusive structures in the southern Primorye region in the Far East. Russ. J. Pac. Geol. 7 (2), 107–123, doi:10.1134/S1819714013020061.

Nevolin, P.L., Utkin, V.P., Mitrokhin, A.N., 2014. Granite formation in a continental crust: dynamics of tectonic positioning and structurization of intrusions (a case study for Primorye, Russia) [in Russian]. Vestnik KRAUNZ, No. 23 (1), 231–246.

Nokleberg, W.J., Parfenov, L.M., Monger, J.W.H., Norton, I.O., Khanchuk, A.I., Stone, D.B., Scotese, Ch.R., Scholl, D.W., Fujita, K., 2000. Phanerozoic tectonic evolution of the Circum-North Pacific. U.S. Geological Survey Professional Paper 1626.

Parfenov, L.M., Khanchuk, A.I., Prokopiev, A.V., Timofeev, V.F., Berzin, N.A., Obolensiy, A.A., Badarch, G., Tomurtogoo, O., Belichenko, V.G., Dril, S.I., Kuz'min, M.I., Bulgatov, A.N., Kirillova, G.L., Rodionov, S.M., Nokleberg, W.J., Ogasawara, M., Scotese, C.R., Yan, H., 2010. Tectonic and metallogeny model for Northeast Asia. Geological Survey Professional Paper 1765.

Panichev, A.M., Popov, V.K., Chekryzhov, I.Yu., Golokhvast, K.C., Seredkin, I.V., 2012. Kudurs of paleovolcano Solontsoviy in the Tayojnaya river basin, East Sikhote-Alin. Uspekhi nauk o zhizni, No. 5, 7–28.

Pavlyutkin, B.I., Chekryzhov, I.Y., Petrenko, T.I., 2016. Problems of Paleogene–Neogene stratigraphy of the Zerkal'naya depression, East Sikhote Alin. Russ. J. Pac. Geol. 10 (4), 283–298, doi:10.1134/S1819714016040072.

Popov, V.K., Grebennikov, A.V., 1997. Geological and geochemical correlation of rhyolites from Yakutinsya and Avgustovskaya volcanic structures, Primorie. Russian Journal of Pacific Geology 13, 583–600.

Popov, V.K., Grebennikov, A.V., 2001. New data on the age of effusives from the Bogopolsky suite in Primorye. Tikhookeanskaya Geologiya, No. 3, 47–54.

Pospelov, G.L., 1973. Paradoxes, Geological-physical Nature, and Mechanisms of Metasomatism [in Russian]. Nauka, Novosibirsk.

Robinson, F.A., Bonin, B., Pease, V., Anderson, J.L., 2017. A discussion on the tectonic implications of Ediacaran late- to post-orogenic A-type granite in the northeastern Arabian Shield, Saudi Arabia. Tectonics 36, doi:10.1002/2016TC004320.

Sakhno, V.G., Akinin, V.V., 2008. First U–Pb Dating of Volcanics from the East Sikhote-Alin Belt. Dokl. Earth Sci. 418 (1), 32–36, doi:10.1134/S1028334X0801008X.

Sakhno, V.G., Rostovskii, F.I., Alenicheva, A.A., 2010. U–Pb isotope dating of igneous complexes from the Milogradovo gold-silver deposit (Southern Primor'e). Dokl. Earth Sci. 433 (1), 879–886, doi:10.1134/S1028334X1007007X.

Sakhno, V.G., Kovalenko, S.V., Lyzganov, A.V., 2016. Granitoid magmatism in the Arminskii block of Central Sikhote Alin (Primorye, Far Eastern Russia): U–Pb geochronology, $^{3}He/^{4}He$ isotopy, petrochemistry, and ore mineralization. Dokl. Earth Sci. 466 (2), 123–129., doi:10.1134/S1028334X16020239.

Sakhno, V.G., Kovalenko, S.V., 2018. Igneous Complexes of the Orochenka Caldera of the East Sikhote-Alin Belt: U–Pb (SHRIMP) Age, Trace and Rare Earth Element Composition, and Au–Ag Mineralization. Dokl. Earth Sci. 479 (2), 420–424, doi:10.1134/S1028334X18040086.

Sidorenko, A.V. (Ed.), 1969. The Geology of the USSR. Primorskiy Kray. Geologicheskoe Opisanie XXXII (1) [in Russian]. Nedra, Moscow.

Sun, S.S., McDonough, W.F., 1989. Chemical and isotopic systematics of oceanic basalts: implications for mantle composition and processes, in: Saunders, A.D., Norry, M.J. (Eds.), Magmatism in the Ocean Basins. Geological Society of London Special Publication 42, 313–345.

Tang, J., Xu, W., Niu, Y., Wang, F., Ge, W., Sorokin, A.A., Chekryzhov, I.Y., 2016. Geochronology and geochemistry of Late Cretaceous–Paleocene granitoids in the Sikhote-Alin Orogenic Belt: Petrogenesis and implications for the oblique subduction of the paleo-Pacific plate. Lithos 266–267, 202–212, doi:10.1016/j.lithos.2016.09.034.

Tsutsumi, Y., Yokoyama, K., Kasatkin, S.A., Golozubov, V.V., 2016. Ages of igneous rocks in the southern part of Primorye, Far East Russia. Memoirs of the National Museum of Nature and Science 51, 71–78.

Utkin, V.P., 1980. Fault Displacement and Their Research Procedure [in Russian]. Nauka, Moscow.

Utkin, V.P., 2005. Structure, geochronology, and structural-dynamic conditions of the vertical development of the East Sikhote-Alin. Magma-metallogenic belt. Dokl. Earth Sci. 405 (8), 1136–1140.

Utkin, V.P., 2013. Shear structural paragenesis and its role in continental rifting of the East Asian margin. Russ. J. Pac. Geol. 7 (3), 167–188, doi:10.1134/S181971401303007X.

Vetrennikov, V.V., 1976. Geological structure of the Sikhote-Alin Natural Reserve and Central Sikhote-Alin Mountains, in: Trans. of the Sikhote-Alin Natural Reserve [in Russian]. Vol. 6.

Watson, E.B., Harrison, T.M., 1983. Zircon saturation revisited: temperature and composition effects in a variety of crustal magma types. Earth and Planetary Science Letters 64, 295–304.

Wiedenbeck, M., Allé, P., Corfu, F., Griffin, W.L., Meier, M., Oberli, F., von Quadt, A., Roddick, J.C., Spiegel, W., 1995. Three natural zircon standards for U-Th-Pb, Lu-Hf, trace element and REE analyses. Geostand. Newslett. 19, 1–23.

Whalen, J.B., Currie, K.L., Chappell, B.W., 1987. A-type granites: geochemical characteristics, discrimination and petrogenesis. Contrib. Mineral. Petrol. 95, 407–419.

Zhao, P., Jahn, B.-M., Xu, B., 2017. Elemental and Sr-Nd isotopic geochemistry of Cretaceous to Early Paleogene granites and volcanic rocks in the Sikhote-Alin Orogenic Belt (Russian Far East) and their implication on regional tectonic evolution. J. Asian Earth Sci. 146, 383–401, doi:10.1016/j.jseaes.2017.06.017.

Zharikov, V.A., 1996. Certain aspects of granite formation. Vestnik MGU. Geology. Issue 4, 3–12.

Editorial responsibility: N.N. Kruk